International Conference on Space Optics—ICSO 2024

Antibes Juan-les-Pins, France 21-25 October 2024

Edited by Philippe Kubik, Frédéric Bernard, Kyriaki Minoglou and Nikos Karafolas

Preliminary STOP Analysis of the Venus Emissivity Mapper instrument





Preliminary STOP Analysis of the Venus Emissivity Mapper instrument

Martin Pertenais^a, Marlene Bamm^{a,c}, Denis Grießbach^a, Simone del Togno^b, Matthias Lieder^a, Simone Arloth^a, Moritz Adams^c, Tom Theisen^c, Markus Czupalla^c, Till Hagelschuer^a, Gisbert Peter^a, and Jörn Helbert^b

^aInstitute of Optical Sensor Systems, German Aerospace Center (DLR), Rutherfordstr. 2, 12489 Berlin, Germany

^bInstitute of Planetary Research, German Aerospace Center (DLR), Rutherfordstr. 2, 12489 Berlin, Germany

^cFH Aachen, Hohenstaufenallee 6, 56064 Aachen, Germany

ABSTRACT

The Venus Emissivity Mapper (VEM) instrument (on EnVision called VenSpec-M), is a multispectral imager for mapping of the Venus surface and its lower atmosphere. This is realized by observation through narrow-band atmospheric windows present in the near-infrared spectral region. VEM will allow to detect thermal emissions like volcanic activity, surface rock composition, water abundance and cloud formation over Venus' surface. The optical design of the instrument includes a single lens imaging Venus's surface on a filter assembly composed by 14 individual filter stripes, and a 2-lenses relay optic re-imaging this spectrally filtered image onto an InGaAs detector. Considering the low intensity level of the scientific signal the instrument is a iming to detect, any external contributor to the effective S ignal to N oise R atio has to be s tudied and if p ossible mitigated. One of the major contributors is, as in most optical instruments, the straylight. The sources of this disturbance signal on the detector are various: e.g. the Sun, solar system bodies (moon, other planets), a mechanical part of the S/C, internal reflections inside the instrument, scattering effects. This paper will first describe the rationale behind the stravlight requirement derivation based on simulated instrument performance and the design features implemented in the instrument to mitigate the straylight effects such as optical b affle, black coatings, diaphragms. In a second part, the straylight analysis performed using this design against the defined requirement will be presented. This includes both ghost images, in-field straylight and off-field straylight. The results of this analysis will finally be compared to the requirements and the design validity assessed.

Keywords: STOP, performance, thermal, structural, Venus, VEM, VERITAS, EnVision

1. INTRODUCTION AND MOTIVATION

1.1 Instrument Description

The Venus Emissivity Mapper (VEM), also called VenSpec-M, is an infra-red push-broom spectrometer developed at DLR for both VERITAS¹ (NASA Discovery Mission) and EnVision² (ESA Cosmic Vision M6 Mission). Thanks to its very high temperature, the thermal emissions of Venus' surface occurs at relatively short wavelengths compared to what we are used to on Earth, namely around 1µm. Luckily, most of these wavelengths happen to be within the atmospheric spectral window. It is therefore possible to map the thermal emissivity of Venus' surface from orbit with VEM, at least on Venus night side. Thus, VEM will operate exclusively while on the night side of Venus.³

The full instrument description and current development status is described in Ref. 4.

The large optical field of view (FoV) of the instrument, about 45°x30°, is imaged by a single lens objective onto a filter assembly. This filter assembly is composed by 14 individual filter stripes featuring narrow band spectral coatings ranging from 790nm to 1510nm. The filter stripes are organized so that one stripe is orthogonal

Further author information: martin.pertenais@dlr.de

to the velocity vector of the S/C projected on the planet surface, such that it creates a push-broom spectrometer strategy. An optical relay of 2 lenses is then used to project the image of this filter assembly onto an InGaAs detector. The detector is thermally controlled by an integrated TEC linked to a S/C Cold Finger. The data from the analogue chain behind the detector is processed by the control unit below the optical barrel in the electronic box. A 2-stage baffle assembly is present in front of the optical barrel: a vaned baffle cone used for straylight measures, and a white painted shield protecting the instrument from too high temperatures and making the mechanical link to the S/C exterior panel.

1.2 STOP Analysis Purpose

The term STOP analysis stands for Structural-Thermal-Optical-Performance Analysis. This is a standard analysis process used in the optical instrumentation design phase to verify the end-to-end design and performances of an instrument.^{5,6} It allows to combine structural and mechanical loads and estimate their impact on the optical performance of an instrument.⁷

In the case of VEM, it is expected that both thermal and structural loads will drive the complete design of the instrument. From a structural point of view, our instrument will fly to space, and therefore need to survive classical mechanical loads from the rocket launch, pyrotechnic shocks, and gravity release effects. On top of that, from a thermal point of view the instrument is placed on two S/C flying to Venus where a very hot thermal environment will dramatically heat up the instrument.

1.3 Requirements

As described in Ref. 8, the main scientific requirements for VEM are the spatial resolution of the images of Venus' surface, the surface coverage with a large FoV, and finally high Signal to Noise Ratio (SNR) in the required spectral bands. For this STOP analysis⁹ exercise, the main three requirements chosen to be analysed are described in Table 1.

Title Req. # Requirement Justification VEM-SYS-PSF Size 90% of the PSF Ensquared En-Direct impact on the Ground Resolved 8340 ergy shall fit in a square smaller Distance (GRD) than or equal to 150µm (TBC) half distance VEM-SYS-Focal The effective focal length shall be Needed to achieve the Ground Sam-10845 Length f = 16.4 mm + / - TBDpling Distance (GSD) and to reach the requirement surface coverage VEM-SYS-Distortion The geometrical distortion shall Limit the impact on the effective GSD 11203 be less than 10% at the edge of and the complexity of the data processthe FOV

Table 1. Requirements to analyse with the STOP analysis.

The first requirement has a direct impact on the Ground Resolved Distance (GRD) and is linked to the optical quality of the design. The Ensquared Energy Distance Requirement is a figure of merit used to characterize the size of a PSF. In this case, 90% of the energy fraction are required to be focused in a square of half distance 150µm. This distance can be directly analysis in any optical design software like OpticStudio Zemax in our case. Note that this requirement is still under discussion and probably going to be modified in the future.

The second requirement is on the absolute value of the effective focal length of the instrument and its acceptable tolerance. One on side, a smaller focal length automatically means a larger field of View for a given detector size. Having a smaller focal length would therefore increase the surface coverage science requirement. However, this would also induce a reduction of the Ground Sampling Distance (GSD). The GSD is the projection of an instrument pixel onto Venus surface in this case. Note that the tolerance on the design value of 16.4mm is not yet determined at the time of the analysis. Actually, the STOP analysis will be in this case used as input to determine the acceptable tolerance on this requirement.

Finally, the last requirement considered for this STOP analysis is the geometrical distortion of the instrument. The requirement states it has to remain smaller than 10% at the edge of the field of view. This is needed on one side to avoid too complex data processing. It would indeed induce a complex spectral and spatial mapping of each pixel, not following the natural lines and columns of the detector. On the other side, the geometrical distortion has a direct impact on the GSD. Section 2.5 will describe the equations behind it in more detail, as the effective GSD is computed based on the pixel size and focal length (as seen for the previous requirement) but also on the geometric distortion that can effectively reduce the real GSD.

2. STOP TOOL AND INPUTS

2.1 Thermal Model

The first input needed for the STOP analysis is a detailed thermal model of the instrument. The thermal concept of the instrument is presented in Fig. 1. The thicker the zigzag lines, the stronger the thermal conductivity is between sub-systems in the instrument. The main goal of this design is to isolate the optical unit and FPA as much as possible from the other major temperature sources. On one side, the baffle assembly receives strong radiative fluxes from the Sun and Venus, on the other side, the electronic box intrinsically generates a significant amount of heat.

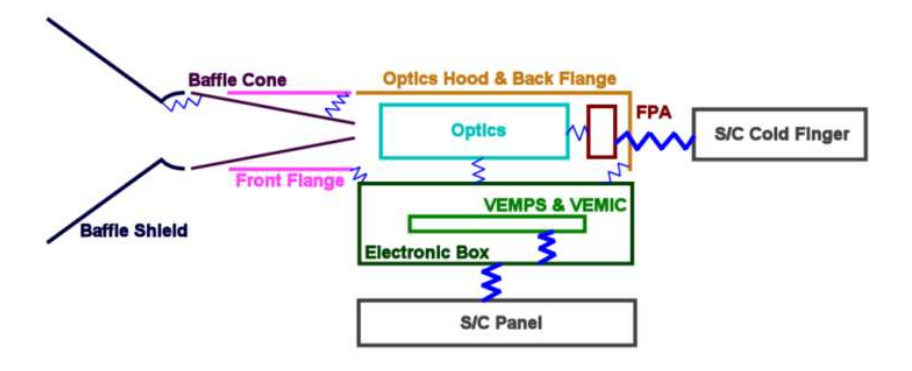


Figure 1. Thermal design concept of the instrument.

Based on the CAD model of the instrument, the detailed thermal model of the instrument was created with ESATAN - Thermal Modeling Suite (ESATAN-TMS). Each component, surface or sub-system was assigned a given set of thermal properties such as linear conductivity or radiative conductivity. The Finite Difference Method (FDM) was used to sample the instrument as well as possible in nodes that can then be associated to a given computed temperature.

2.2 Structural Model

Similarly to the thermal modeling, a structural model was created using the software FEMAP, see Fig. 2. Each surface and sub-system of the instrument is again sampled in numerous nodes that are assigned to given mechanical properties. Such a model can then be used for a Finite Element Model (FEM) analysis where mechanical loads can be applied to the interface points and propagated inside the instrument. Structural deformation for each node can then be estimated and analysed.

It has to be noted here, that the structure model at the time of the analysis was preliminary. For example, the structural model of the optical sub-system was not yet available to the instrument team. The three lenses were therefore simply attached as Rigid Body Elements (RBEs) directly on the mechanical barrel around them. This automatically constraint them completely in their rotational motion.

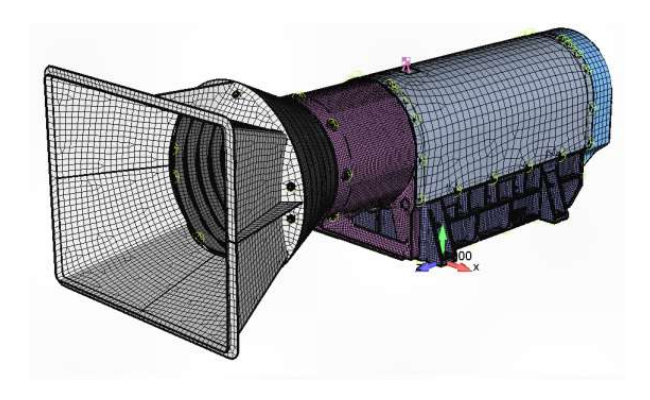


Figure 2. Structural FEM model of VEM in FEMAP software.

2.3 Optical Model

Finally, the last branch of modeling needed as input for the STOP analysis is the optical design. For the VEM project case, the optical design is performed with OpticStudio Zemax software and is the responsibility of LESIA in Meudon (France). Figure 3 shows a screenshot of the 3D optical design and the associated lens data. The Zemax file will be directly used as input in the STOP Tool described in Section 2.4, and needs to be prepared in a given specific format.



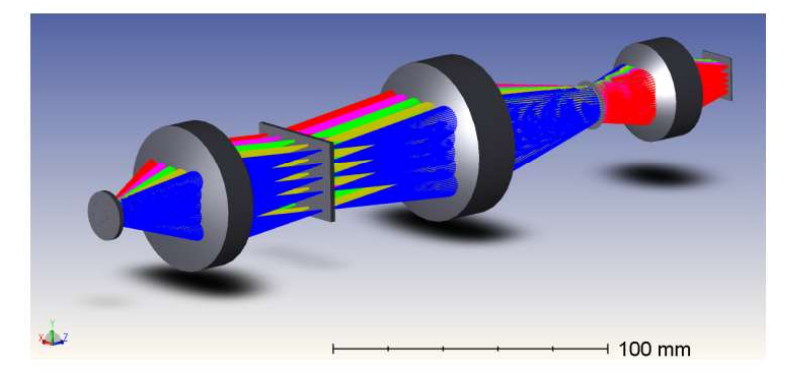


Figure 3. Optical design model of VEM.

2.4 STOP Tool description

In collaboration with the Institute of Optical Sensor systems at DLR Berlin, the FH Aachen is developing its own STOP Analysis Tool. Figure 4 presents the overview of this tool's structure.

After the thermal analysis has been performed and the model prepared accordingly, the first step of the process is to perform the mapping from the thermal model to the structural one.¹⁰ This can be done with the so-called Thermal Mapping Tool (TMT) or manually by the operator in FEMAP, as described in more detail in Section 3.2. The structural analysis can then be performed using these thermal loads as inputs. At this stage, deformation maps can be created as output, including both thermal and structural loads as disturbances sources.

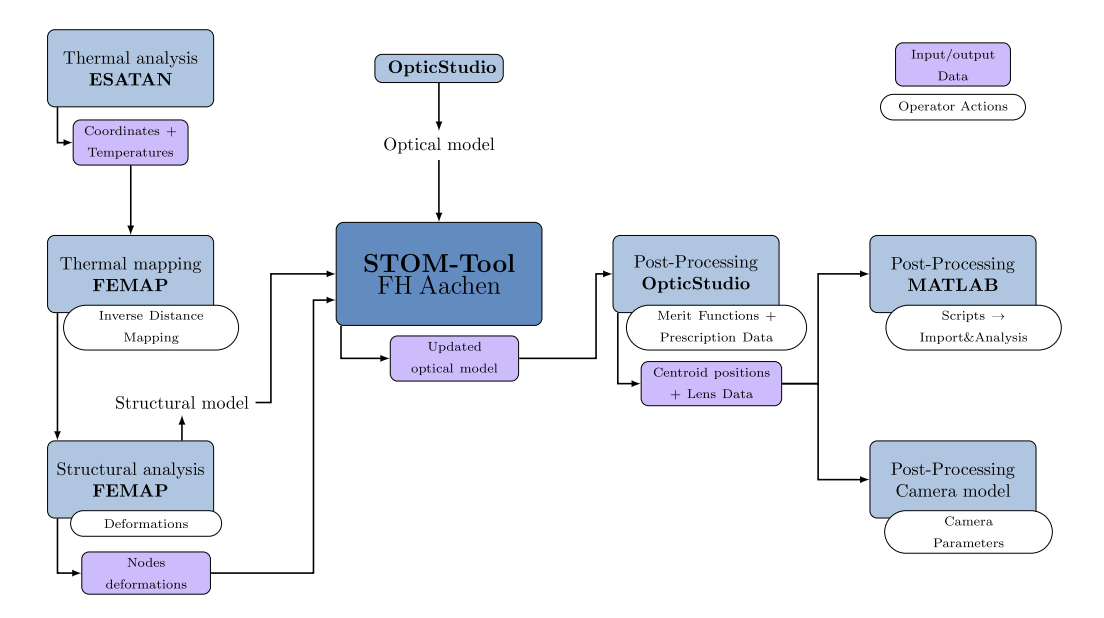


Figure 4. End-to-end flow diagram of the STOP Analysis process performed.

The next step in the process is to link these deformation maps with the optical model in Zemax. A polynomial fitting is needed for each optical surface that can then be applied to the relevant surfaces in the optical model prepared as input. On top of this surface deformation maps, the absolute position of each surface can be modified in case it was impacted by the thermo-mechanical disturbances. Eventually, an updated optical model is created and provided as output. From this optical model, pre-defined merit functions or macro script can be run automatically to extract performance information on optical parameter (e.g. PSF size, centroid positions of PSFs, distortion value, focal length value,...). This data can then be processed either with separate scripts in Matlab or Python for example or used to feed the camera model described in the next section.

2.5 Camera Model

Any imaging optical instrument can be modeled by a geometrical camera model. Such a model allows to compute the transformation from an the direction of an object in front of the instrument to the expected centroid position of its image on the detector. A short description of the model structure is described here:

To map a direction vector, given with $(X, Y, Z)^T$ in some World Reference Frame (W-RF), it first needs to be transformed to the camera Boresight (BS)-RF with

$$\begin{pmatrix} X \\ Y \\ Z \end{pmatrix}^{BS} = \mathbf{R}_W^{BS} \begin{pmatrix} X \\ Y \\ Z \end{pmatrix}^W, \tag{1}$$

where $\mathbf{R}_W^{BS}(\omega,\varphi,\kappa)$ is the exterior orientation of the camera BS-RF w.r.t the W-RF. Considering projective geometry, the normalized camera coordinate $(x,y)^T$ can be recovered by dividing the homogeneous coordinate $(xZ,yZ,Z)^T$ by its non-zero factor -Z. This can be seen as a projection to a virtual plane at Z=-1, being the normalized detector plane.

2.5.1 Interior Orientation

By definition the optical axis is perpendicular to the detector plane. The pixel coordinate $(u, v)^T$, given in the detector-RF is now determined from the boresight coordinates with

$$\begin{pmatrix} u \\ v \\ 1 \end{pmatrix} = \mathbf{K} \begin{pmatrix} x \\ y \\ 1 \end{pmatrix}, \tag{3}$$

where the camera matrix K represents a pinhole camera model, containing the principal point $(u_0, v_0)^T$ and the effective focal length $f_{\lambda} = f_0 + a + b\lambda + c\lambda^2$, which in this context is the wavelength dependent distance of the perspective centre (pinhole) to the detector.

$$\mathbf{K} = \begin{bmatrix} f_{\lambda} & 0 & u_0 \\ 0 & f_{\lambda} & v_0 \\ 0 & 0 & 1 \end{bmatrix} . \tag{4}$$

The principal point, as used here, is the point where the optical axis intersects with the detector. It is given w.r.t. the origin of the detector-RF.

2.5.2 Distortion Model

Since the pinhole model does not consider geometric distortion, it is extended by the Brown-Conrady model. It consists of a radial-symmetric component δ_r , describing pincushion/barrel distortion, and a tangential component which is omitted in this case. Normalized boresight coordinates are corrected as follows.

$$\begin{pmatrix} x_d \\ y_d \end{pmatrix} = \begin{pmatrix} x \\ y \end{pmatrix} + \boldsymbol{\delta}_r(x, y, \boldsymbol{k})$$
 (5)

The radial-symmetric model with the radial distance $r^2 = x^2 + y^2$ is expressed as

$$\boldsymbol{\delta}_r(x, y, \mathbf{k}) = \begin{pmatrix} x \\ y \end{pmatrix} (k_1 r^2 + k_2 r^4 + k_3 r^6 + \cdots).$$
 (6)

The set of parameters defined here, can be calibrated either by simulation using some centroids measurements with an optical design software (like for this exercise here with OpticStudio Zemax), or by an actual measurement with hardware. As soon as these parameters are estimated, it is very effective to use this camera model to estimate performance and sensitivity impacts of the instruments. Section 3.3.3 at the end of the paper will show a concrete example.

3. ANALYSIS AND RESULTS

3.1 Test Cases

A pure structural load case was used as a test case: gravity release. A typical 9.807m/s^2 load was applied sequentially on the three axis of the instrument to check the impact on the optical performances. As expected its impact is negligible, but this case was used mostly to validate the interfaces between the different models.

In order to have the full STOP loop covered, four thermal cases were defined within the operational range of the optics of [0°C;+40°C]. The data was extracted from the steady state analysis of the thermal model done with ESATAN-TMS.

- Cold Case In this case, the optical elements are all very close to 0°C, their minimal operational requirement authorized.
- Hot Case The other extreme of the operational range is covered by this case, with optics temperature close to +40°C.

- Temperate Case this case provides an intermediate case between the two extreme ones, with optics temperature close to the middle of range at +20°C. This case will be used in Section 3.3.3 as the nominal case for the sensitivity analysis of the parameters.
- **Verification Case** Finally, a fourth was defined with temperature data in an other intermediate case around +30°C. This case will **not** be analysed with the STOP Tool, but used as reference to validate the integrity of the sensitivity table described in Section 3.3.3. This will confirm the possibility to predict parameter values by interpolating within the operational range.

The details of the average temperature of the several optical elements are presented in Table 2 for the different input cases.

Table 2. Average temperatures for the difference input cases, in °C							
Temperature cases	Temperate	Cold	Hot	Verification			
Lens 1	21.7	7.0	38.3	29.7			
Filter	21.6	7.0	38.2	29.7			
Lens 2	21.6	7.1	38.1	29.6			
Lens 3	21.6	7.5	37.8	29.3			
Average	21.6	7.2	38.1	29.6			
Difference to Temperate Case	0.0	-14.5	+16.5	+8.0			

3.2 Mapping and Fitting

3.2.1 Thermal-Structural Mapping

The first step in the STOP process described in Fig. 4 is to map the thermal model onto the structural model. As the thermal mapping tool (TMT) from the software was not ready at the time of this analysis loop, this step was performed manually using the software FEMAP. The method here is to associate each structure node to a thermal node, and more importantly to perform some kind of interpolation for the structural nodes not directly available in the thermal model. The thermal model indeed has a lower surface sampling and number of nodes. The Inverse Distance Weighting method is used in FEMAP to compute temperatures values based on the distance of the node to the closed thermal nodes available and associated weighting factors. Considering the facts, that some sub-systems in the instrument are physically close to each other but thermally decoupled, much more accurate results were obtained by repeating this exercise at sub-system level, instead of trying to map the whole instrument at once.

The results of the group mapping are presented in Fig 5 for the hot thermal case.

In order to have a more quantitative assessment of the mapping quality, the temperature differences for each relevant component has been computed. For each component, the minimum, maximum and average temperatures have been compared between the reference thermal model and the model mapped with the structural model. Table 3 presents the results of this comparison.

The results are excellent using this method, with for all the cases less than 1°C difference between the mapped temperature and the reference one in the thermal model. With the exception of the Baffle Shield, the mounts and the electronic box, all the sub-systems are actually within 0.1°C from the reference.

3.2.2 Deformation Fitting

Using the mapped thermal model on the structural model, the structural FEM analysis can be performed for the cases defined in Section 3.1. For each case, the output of the analysis is a NASTRAN PUNCH (pcf) file containing the deformation value for each node included in the model. The key part of the STOP analysis is to fit these deformations of each node to the optical model. With the use of empty coordinate breaks around each optical surface, as seen in Fig. 3, and a change of surface type in OpticStudio of said surfaces, the STOM-Tool

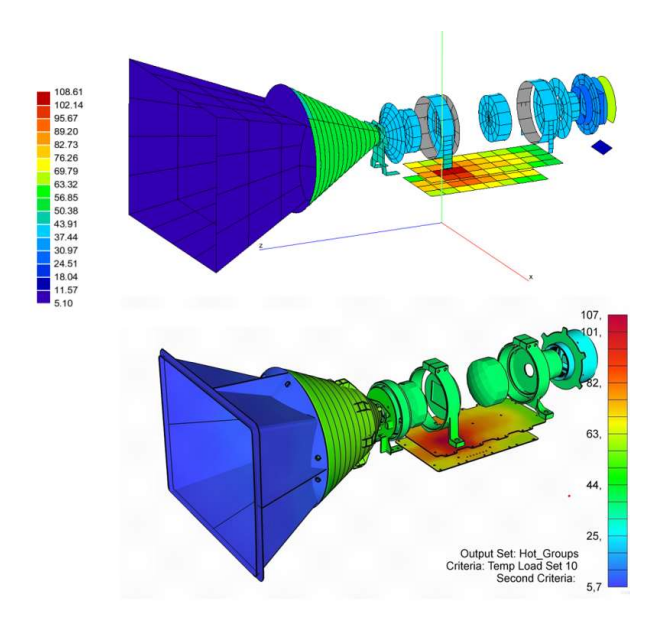


Figure 5. Thermal mapping of the structural model for the hot thermal case. The top image shows the thermal model of VEM in ESATAN, and the bottom omage the achieved mapping on the structure model in FEMAP, using the group mapping method.

TD 11 0	TD .	1. CC				c	. 1	1 .	.1 1	
Table 3	Temperature	differences	using th	e group	manning	tor 1	the	hot.	thermal case	
Table 0.	Tomporadare	CHILCI CHICCE	aniing on	CSICUP	mapping	TOT (ULL	1100	uncilian case.	•

Component	Absolute Difference (°C)				
	Min. Temp.	Max. Temp.	Avg. Temp.		
Lens 1	0.0001	0.0024	0.0012		
Filter	0.0000	0.0000	0.0000		
Filter Wedge	0.0022	-0.0020	-0.0002		
Lens 2	0.0005	-0.0002	0.0001		
Lens 3	0.0001	-0.0001	0.0002		
Sensor	0.0000	0.0000	0.0000		
Baffle Shield	0.5753	-0.3358	0.2173		
Barrel	0.0001	0.0000	0.0679		
Barrel Mount	0.0001	-0.3188	-0.4784		
E-Box	0.1361	-0.0461	-0.0273		

is fitting a Zernike polynomial function on top of each surface and computing displacement values and rotations for all of them. Figure 6 shows an example of visual verification for the fit quality of one surface.

In this example, for the surface of one lens in the optical system, the modified surface in the optical model (using the polynomial function and the rigid body deformations) is shown in 3D on top of the reference one in the deformed structural model. On the right-hand side of the figure, the delta map between these 2 surfaces is computed. The core of the tool is eventually to compute rigid body deformation (coordinate breaks translations and rotations) and polynomial coefficients to minimize this delta map. Finally, when the fitting for all the surfaces is successful, an updated optical model in form of a new OpticStudio Zemax file is created and saved. In case of transient analysis (not performed for this loop), the same process is applied but with time series as inputs instead of static models. Temperature and deformation evolution can be plotted and visualized in the tool, and a configurable number of optical models can be exported.

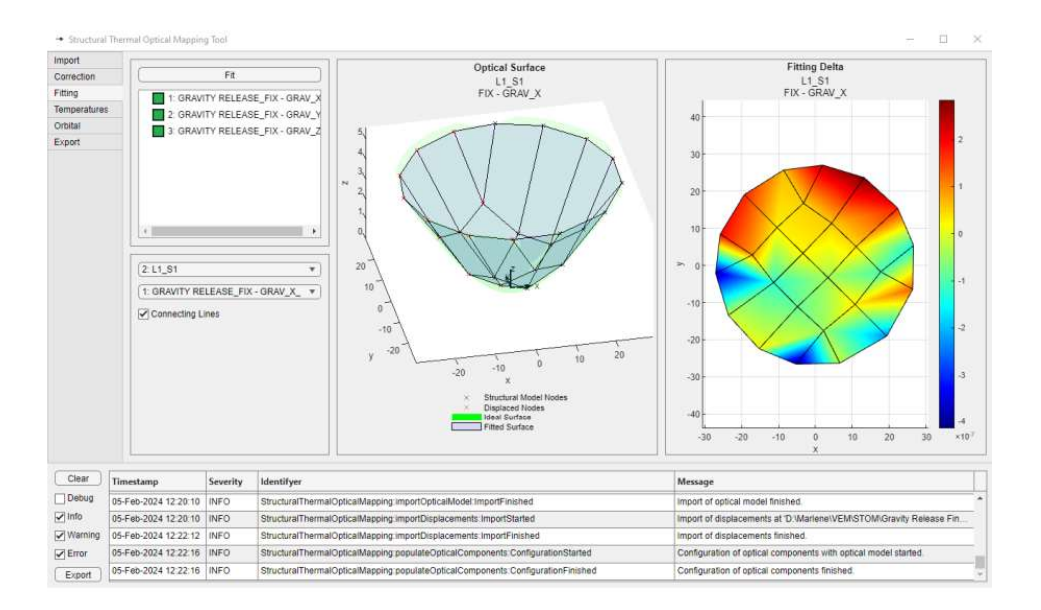


Figure 6. STOM tool - Fitting tab

3.3 Data Analysis

3.3.1 Data Extraction from Zemax

The exported Zemax files from the STOM tool are analysed in a similar way than the original nominal file. In that way, a comparison of pre-chosen parameters can be performed to help draw conclusions on the requirements and/or design validation. To ensure this, pre-defined merit functions were created to read and save the chosen parameters. In our example for VEM, the following optical parameters were read in Zemax in the pre-defined merit functions:

- CENX and CENY For each of the pre-defined FoV points, the centroid of their image on the detector and on the filter assembly intermediate image was saved via these operands. Figure 7 shows for example the exaggerated centroid displacements on the detector for the three thermal cases.
- **GENC** This operand in Zemax computes the size of the square on the detector for a given FoV position needed to fit the pre-defined % of energy of the PSF. In other words, it provides the size of the PSF, to verify requirement VEM-SYS-8340
- WFNO and EPDI These two parameters correspond to the working f-number of the instrument and the entrance pupil diameter, and are dependent on the wavelength. The product of both value provides, per definition, the effective focal length of the system for a given wavelength used to verify requirement VEM-SYS-10845
- Lens Parameters some key parameters such as surface radii, lenses inter-distances, relative rotation angles between lenses are directly read in Zemax and can be used during the analysis as reference values.

These are of course just examples of parameters that can be extracted from the modified optical model. Depending on the project needs and of the loads simulated, any available parameter in the optical software could be read and extracted. Typical other useful parameters could be the Modulation Transfer Function (MTF), the vignetting, the actual aberration (e.g. spherical aberration, astigmatism, coma) values, the chromatism, the polarization sensitivity.

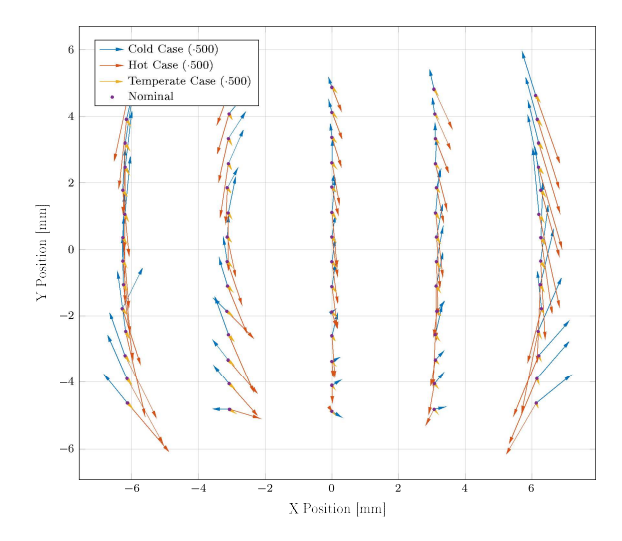


Figure 7. PSF Centroid displacements on the detector across the FoV, with a factor 500 exaggeration of the arrows for visualisation purposes

3.3.2 Analysis and requirement verification

Using the Ensquared Energy values of the PSFs directly extracted from Zemax with the pre-defined merit functions, the verification of the requirement is straight-forward, such as the impact of the thermal cases on it. Figure 8 present the results for the three thermal cases. Each bundle of rays corresponds to one spectral filter that is sampled with five FoV positions along it. The first observation is that in any case, the requirement of 150µm half distance for 90% of the PSF energy is met, as all the curves remain below the 300µm full distance. The impact of the temperature appears to be very small if not negligible. Depending on the spectral filter, and on the position inside the FoV the cold or the hot case are the worst cases. In general, the impact between the two extremes remain limited to less than 5%.

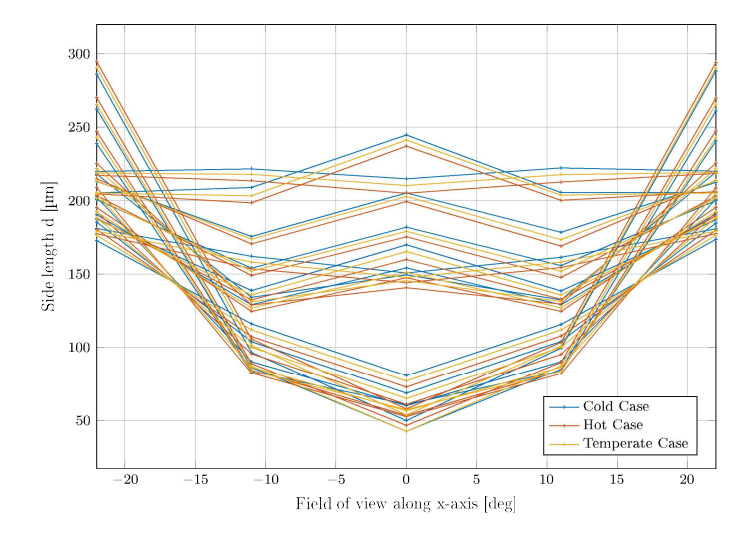


Figure 8. Ensquared Energy Distance for 90% of the PSF size. Each bundle of 3 colored rays (cold, hot and temperate case) represent the PSF size for one spectral filter, computed for the correct wavelength and position on the FoV in the along track direction. The X axis corresponds to the other axis of the FoV.

Using the centroid values exported from the output Zemax files, the camera model described in Section 2.5 was created. This model is providing values of its different parameters for each of the cases ran through the STOP analysis: the focal length, the distortion parameters and the optical axis interface with the detector. These values of effective focal length over wavelength for each of the thermal cases, and distortion parameters over the FoV angle, are used to verify the requirements listed in Section 1.3. The raw Zemax computation was also plotted on top of the modelled values for validation of the model. Figure 9 shows again that spectral variation of the focal lengths dominates strongly compared to the variation with temperature. The same applies to the geometric distortion in Fig. 10, where the distortion model seems to be independent from the thermal case, and well within the requirement of 10%.

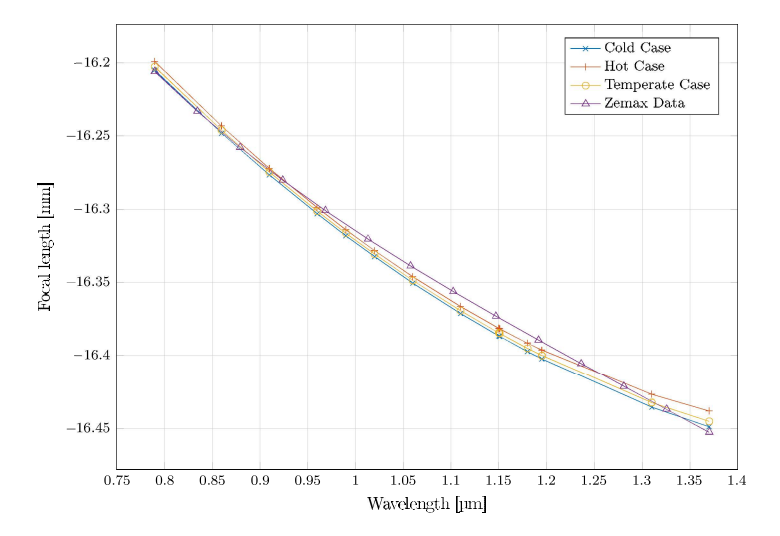


Figure 9. Effective focal length of the instrument as a function of the wavelength, computed for each of the thermal cases simulated. The purple curve on top is the direct output of Zemax, used for model validation.

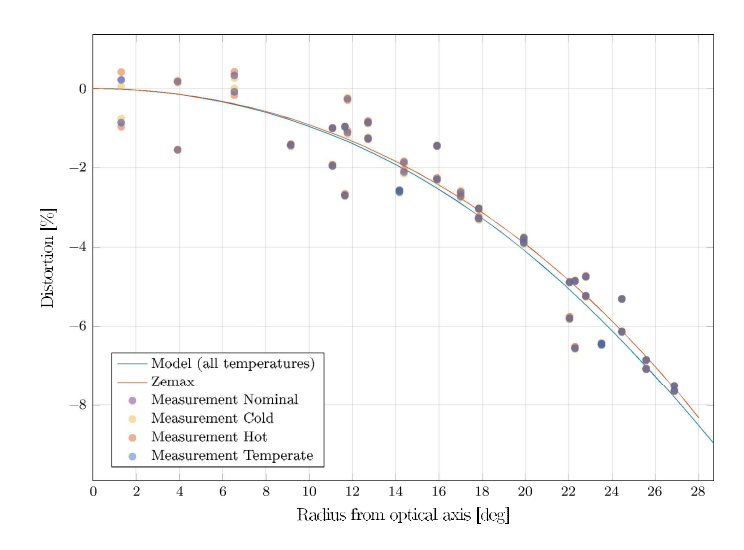


Figure 10. Geometrical Distortion of the instrument as a function of the angular distance to the optical axis, computed for each of the thermal cases simulated. The red curve on top is the direct output of Zemax, used for model validation

The centroid displacements showed in Fig. 7 are computed in comparison with the thermal nominal case at

20°C. Depending on the position on the detector, they vary between 1µm and 6µm for the hot case, and 0.5µm and 4µm for the cold case. With the help of the camera model, these displacements can be traced back to change of the optical axis position with respect to the detector. Looking at the lens parameter data extracted from Zemax, physical translation of the lenses compared to the detector are observed, in the positive direction along Y for the hot case, and in the negative direction for the cold case. This is the consequence of the heat propagation through the system, that was applied during the thermo-structural analysis.

3.3.3 Sensitivity Analysis

Using the values obtained for different thermal cases (nominal, hot, temperate and cold), it could be verified that all the parameters from the camera model were behaving linearly with temperature. Based on this assumption, sensitivity values for each these parameters were derived, as seen in Table 4. The sensitivity values were computed independently using either the hot case or the cold case, against the temperate one as reference. We considered the results close enough to simply compute the mean value of the two results to define the final sensitivity value to be used.

Par	ameter	Cold	Hot	Average
f_0	[px/K]	0.0050	0.0046	0.0048
u_0	[px/K]	0.0005	0.0002	0.0004
v_0	[px/K]	-0.0083	-0.0082	-0.0083
a	[px/K]	0.0519	0.0966	0.0743
b	$[px/\mu mK]$	-0.1018	-0.1908	-0.1463
\mathbf{c}	$[\mathrm{px}/\mu\mathrm{m}^2\mathrm{K}]$	0.0508	0.0967	0.0737

Table 4. Sensitivity values for the camera model parameters, compared to the temperate case.

These parameters allow to estimate temperature impacts on the key parameters of the camera model, without having to re-run the full STOP analysis loop. In order to verify their validity, the so-called verification case was added to the analysis, as described in Section 3.1. In this thermal case, the temperature of the instrument was chosen as far as possible from existing cases, and was not used to determine these sensitivity parameters. Using these sensitivity values, we computed the predicted focal length f_0 , principal points u_0 and v_0 and the wavelength dependent focal length f_{λ} for the temperature of the verification case. These predicted values could be compared to the real values given by the full STOP analysis loop. Table 5 presents the comparison of both analysed and predicted values, as well as the absolute difference between both.

Parameter		Verification Case (Analysis)	Verification Case (Prediction)	Abs. Error
f_0	[px]	-810.1092	-810.1243	-0.0151
u_0	[px]	0.0196	0.0193	-0.0003
v_0	[px]	-0.1070	-0.0998	0.0073
f_{λ}	[px]	-817.1550	-817.1857	-0.0308

Table 5. Verification of the sensitivity parameters with the so-called Verification Case.

The prediction parameters are perfectly matching the analysed one with the STOP analysis, thereby verifying the validity of the use of these simplified sensitivity values for the camera model parameters.

4. CONCLUSIONS

The STOP analysis presented in this paper is still preliminary, and was used as a test case for the on-going development of the STOP Tool at FH Aachen. The structural and thermal model were very preliminary and in many ways not realistic (e.g. lenses attachment, optical barrel interface to the electronic box, some thermal conductivity values, detector).

This work could however prove the feasibility of such a STOP analysis with this homemade tool on a complex instrument like VEM. The thermal mapping onto the structural model was one of the key and more complex part,

as the module in the Tool responsible for it was not available yet. One next step for this work will be to re-run the same analysis, but with the mapping done within this Thermal Mapping Tool, and to compare the results to the manual solution used within FEMAP presented here. The fitting of the thermal and structural deformations onto the optical model was also successfully performed. Both rigid body deformations, and polynomial surface deformation were added and implemented in the optical design, allowing us to use the output Zemax files as basis for performance analysis and comparison to the nominal case. Using the DLR internal geometric camera model? generated based on the Zemax data, sensitivity parameters were defined and computed allowing to estimate impact of thermal cases, without having to re-run a full STOP analysis loop.

As the projects advances in its design phase, this analysis will be repeated with the updated thermal and structural models. A longer list of requirements will be added to the verification cases and some transients run will be simulated, to verify for example the variation of performance across one orbit around Venus.

ACKNOWLEDGMENTS

The authors thank the German federal ministry for economics affairs and climate action for financial support for the STOP Tool development project.



REFERENCES

- [1] S. E. Smrekar, et al., "VERITAS (Venus Emissivity, Radio Science, InSAR, Topography, and Spectroscopy): A Discovery Mission," in [2022 IEEE Aerospace Conference (AERO)], 1–20 (2022).
- [2] A. G. Straume-Lindner, et al., "Science objective and status of the EnVision mission to Venus," *Proc. SPIE* **18247** (2024).
- [3] J. Helbert, et al., "The Venus Emissivity Mapper (VEM): obtaining global mineralogy of Venus from orbit," in [Infrared Remote Sensing and Instrumentation XXVI], Proc. SPIE 10765 (2018).
- [4] T. Hagelschuer, et al, "The Venus Emissivity Mapper (VEM): Instrument design and development for VERITAS and EnVision," in [Infrared Remote Sensing and Instrumentation XXXII], Proc. SPIE 13144 (2024).
- [5] Gracey, R., Bartoszyk, A., Cofie, E., Comber, B., Hartig, G., Howard, J., Sabatke, D., Wenzel, G., and Ohl, R., "Structural, thermal, and optical performance (STOP) modeling and results for the James Webb Space Telescope integrated science instrument module," in [SPIE Astronomical Telescopes + Instrumentation], 99111A (08 2016).
- [6] Tse, L. A., Chang, Z., Somawardhana, R. P., and Slimko, E. M., "Structural, Thermal, and Optical Performance (STOP) Modeling and Analysis for the Surface Water and Ocean Topography Mission," in [48th International Conference on Environmental Systems], Thermal and Environmental Control Engineering Analysis and Software (2018).
- [7] Bolognese, J. and Irish S., "Structural-Thermal-Optical-Performance (STOP) Analysis," *Thermal Fluids Analysis Workshop* (2015).
- [8] J. Helbert, et al, "The Venus Emissivity Mapper (VEM): advanced development status and performance evaluation," in [Infrared Remote Sensing and Instrumentation XXVIII], Proc. SPIE 11502 (2020).

- [9] Marlene Bamm, "Struktur-Thermal-Optische Performanceanalyse des Venus Emissivity Mappers," in [Bachelor thesis], FH Aachen (2024).
- [10] Simon Appel, J. W., [Simulation of Thermoelastic Behaviour of Spacecraft Structures], Springer Cham (2022).
- [11] Brown, D. C., "Close-range camera calibration," Photogrammetric Engineering 37(8), 855–866 (1971).